Cement and Concrete Research 41 (2011) 161–168

Contents lists available at ScienceDirect

Cement and Concrete Research

journal homepage: http://ees.elsevier.com/CEMCON/default.asp

C-S-H/solution interface: Experimental and Monte Carlo studies

Christophe Labbez [a,*], Isabelle Pochard [a], Bo Jönsson [b], André Nonat [a]

[a] ICB UMR 5209 CNRS, Université de Bourgogne, F-21078 Dijon Cedex, France
[b] Theoretical Chemistry, Chemical Center, P.O. Box 124, S-221 00 Lund, Sweden

ARTICLE INFO

Article history:
Received 3 June 2010
Accepted 27 October 2010

Keywords:
B: Calcium-silicate-hydrate (C-S-H)
Surface charge density (C)
Electrokinetic potential (C)
Cation (C)
Adsorption (C)

ABSTRACT

The surface charge density of C-S-H particles appears to be one of the key parameters for predicting the cohesion strength, understanding the ion retention, the pollutant leakage, and admixture adsorption in hydrated cement pastes.

This paper presents a Monte Carlo simulation of the surface-ions interactions that permits the prediction of surface charge density (σ), electrokinetic potential (ζ) and ions adsorption of mineral surfaces in equilibrium with a given electrolyte solution. Simulated results are compared to experimental data obtained by titration, electrokinetic potential measurements and ions uptake in the case of C-S-H suspensions. An excellent agreement is found between simulated and experimental results.

The wide spread idea that calcium is a potential determining ion in cement paste systems appears to be incorrect. Instead, the pH controls the charging behaviour of C-S-H nano-particles. This paper also shows to what extent the electrostatic interactions contribute to the measured Ca/Si ratio.

© 2010 Elsevier Ltd. All rights reserved.

1. Introduction

It is now well established that calcium-silicate hydrate (C-S-H) nano-particles are the main component of the cohesion of cement paste. Attractive forces between them [1–5] lead to aggregation and formation of the network that gives the mechanical and structural properties of the cement paste and of the final concrete construction. Recently, Delville et al. [6,7] and Jönsson et al. [8,9] have shown that this attraction occurring between highly charged C-S-H particles originates from the fluctuation of ion charges in the electric double layer (EDL), so-called ion–ion correlations [10,11]. Hence, the surface charge density of C-S-H particles appears to be one of the key parameters for predicting the cohesion strength [12] and the structure of the final concrete construction. On the other hand, the C-S-H surface charge density is also a determinant factor for understanding the ion retention and transport (diffusion and electro-migration), the pollution leakage, and admixture (polyelectrolytes and polymers) adsorption in cement materials [12–18]. But so far, little is known about the ionization equilibrium of the silanol groups present at the C-S-H/solution interfaces, i.e. variation of the C-S-H surface charge with pH, ion concentration and valency, and so forth.

In a recent paper [19], we have presented a Monte Carlo simulation (MC) method in the Grand Canonical (GC) ensemble [8,20,21], e.g. at constant volume (V), temperature (T) and chemical potential (μ), that permits the simultaneous prediction of surface charge density (σ) and electrokinetic potential (ζ) of mineral surfaces in equilibrium with an arbitrary electrolyte solution. The basic idea of the method is to describe the macroscopic measurable surface charge density of a mineral surface as the sum of the microscopic states of its surface titrable sites interacting between themselves and with the surrounding ions. In a close relation to the "real world", the surface charge density of a mineral is thus determined by the probability to find an ensemble of titrating sites in a deprotonated state. Following this concept, a microscopic model of the solid/liquid interface have been developed and reduced to its more simple form, see Fig. 1. That is, the electrolyte solution is described by the primitive model where the ions are represented as explicit charged hard spheres while the water molecules are implicitly treated through a dielectric continuum. On the other hand, only the titrable sites from the known structure of the mineral surface are explicitly represented by charged or neutral spheres (depending on their ionization state). The electrostatic and hard-core interactions alone are considered in our approach. The electrostatic being the more long-range and dominating interaction, it is thought to be the main physical ingredient of a liquid system or a solid/liquid interface. During our simulations, in addition to the usual stochastic moves of a GCMC simulation (move of ion, exchange of a salt pair with an infinite bath), the surface sites are individually allowed to titrate. The MC simulations technique is described in numerous text books. For a complete description of MC method, see [22]. For each of these moves an associated energy is calculated which involves all hard-core and coulombic pair interactions (ion–ion, site–site, and ion–site). This constitutes the main difference with existing charging process models [14,23–25] where all interactions and titrations are averaged out through a mean field potential using the

* Corresponding author.
E-mail address: christophe.labbez@u-bourgogne.fr (C. Labbez).

0008-8846/$ – see front matter © 2010 Elsevier Ltd. All rights reserved.
doi:10.1016/j.cemconres.2010.10.002

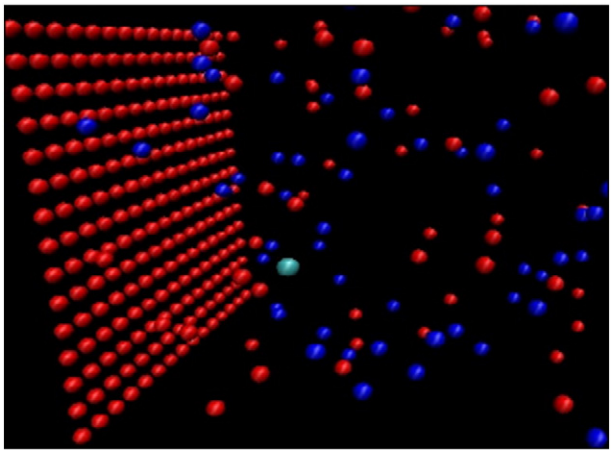

Fig. 1. A slab model of one C-S-H particle in contact with a salt solution. Titrating sites, modelling silanol groups of the C-S-H surface, are treated as discrete and distributed on a square lattice of dimensions 4.56×4.56 Å^2. Sites are allowed to titrate according to the solution pH and composition. In the solution, red, dark blue and light blue spheres represent OH^-, Ca^{2+} and Na^+, respectively.

Poisson–Boltzmann equation. This means that in the latter the ion–ion, ion–site and site–site correlations are neglected. However, as it will be shown in this work, these correlations appear to be essential for the understanding of ion adsorption, electrokinetic behaviour and charge formation of C-S-H particles.

In the particular case of a C-S-H particle, the "macroscopic" surface charge comes from the titration of many individual silanol groups present at the C-S-H/liquid interface. The equilibrium reaction of one particular silanol reads:

$$\equiv Si{-}OH \leftrightarrows \equiv Si{-}O^- + H^+ \quad (1)$$

Following basic thermodynamic and without losing any generality, the intrinsic dissociation constant K_0 of one silanol group corresponding to reaction (1) can be expressed as:

$$K_0 = \frac{a_{SiO} a_H}{a_{SiOH}} \quad (2)$$

Where a_{SiO} and a_{SiOH} are the surface activities of Si–O^- and Si–OH groups respectively and a_H is the activity of the proton. The latter can be rewritten in a more convenient way:

$$\ln\left(\frac{\alpha}{1-\alpha}\right) = -\ln\left(\frac{\gamma_{SiO}}{\gamma_{SiOH}}\right) + \ln 10(pH - pK_0) \quad (3)$$

Which relates the ionization fraction α of an individual silanol group as a function of the activity coefficient γ of its ionised and protonated state, pH ($-log a_H$) and pK_0 ($-log K_0$).

From Eq. (3), one can recognize that the term on the left hand side is the free energy change that we are looking for, e.g. change from deprotonated to protonated state of a silanol group, and the first term on the right hand side is the associated excess free energy change. It follows that the free energy change for titration of a silanol group can be expressed as [26]:

$$\begin{aligned} \Delta U &= \Delta U_{el} + kT\ln 10(pH - pK_0) \quad \text{for protonation} \\ \Delta U &= \Delta U_{el} - kT\ln 10(pH - pK_0) \quad \text{for deprotonation} \end{aligned} \quad (4)$$

Where ΔU_{el} is change in the total electrostatic energy (sum over all species of the system) when a silanol is protonated or deprotonated, k is the Boltzmann constant and T the temperature. These two last equations define the energy for titration used in our Monte Carlo simulations. No additional surface adsorption constant is used. Obviously, within this model (see Eq. (4)), one can notice that ΔU of silanol groups and thus their ionization states depends strongly on the pH and electrostatic interactions ΔU_{el} with the surroundings species. ΔU_{el} is also a strong function of the surface site density, salt concentration and valency, suspension concentration as well as the amount of other charged additives.

As we will show in this work, in addition to have a solid physical basis, the main practical advantage of this new approach is that it reduces the numerous fitting parameters (electric double layer capacitances, effective adsorption constant of ions...) of the classical Stern model [24,25] to two well-defined parameters, namely the density ρ_N and the ionization equilibrium constant pK_0 of surface sites. Here, ρ_N is taken equal to that of the homologue tobermorite structure [27] (4.8 sites/nm²) and pK_0 to that of the first ionization of the silicic acid (9.8).

The aim of this paper is twofold. On the one hand, we will show how this new theoretical approach can improve the description and understanding of the C-S-H/solution interface in terms of charging process, electrokinetic behaviour and ion adsorption. On the other hand, we will try to explain some of the implications of these results for cement chemistry.

The paper is organized as follow: first a brief description of materials and methods is given. Secondly, predicted and experimental results of titration electrophoretic mobility measurements and experimental adsorption isotherms obtained on C-S-H dispersions are presented. After this, the results and their implications for cement chemistry are discussed. Finally some conclusions are drawn.

2. Materials and methods

Since the experimental method and the technical details of our simulations are described elsewhere [19] we shall only give in this paper a brief description of them.

2.1. Experiments

C-S-H mother suspension has been prepared by mixing 5.946 g of analytical grade calcium oxide (Prolabo), 9.724 g of colloidal silica TA92 (Rhodia) and 791.50 g of distilled–deionised milli-Q water. These proportions have been chosen in order to obtain C-S-H of Ca/Si stoichiometric ratio equal to 0.66. The calcium oxide powder has been decarbonated in a furnace at 1000 °C for 4 h. The milli-Q water has been boiled to remove soluble CO_2. Silica has not undergone any treatment. The pH of the obtained suspension is 10.35 and the liquid to solid ratio is 50.0. For the titration experiment, this suspension has been used as it is while it has been diluted hundred times for the electrokinetic measurements.

Titration experiments with C-S-H suspensions were carried out between pH 10.35, the initial pH of our suspension, and 13.5. Care has been taken to prevent contamination of solutions with CO_2. Blank solutions, having the same volume as batches used for the titration experiments, that is 34.3 mL, were prepared to correct for minor CO_2 contamination. The experiments were conducted by adding a known amount of base (NaOH) to both blank solutions and suspensions. Blank solutions and C-S-H suspensions were then aged and vigorously shaken during 3 weeks to ensure a good equilibration. Finally, the pH value and sodium and calcium content of both blank and supernatant solutions of C-S-H suspensions (obtained after centrifugation) were measured with a suitable high alkalinity pH electrode and inductively coupled plasma absorption optical spectroscopy, respectively. The resulting "adsorb" amount of sodium (Na^{ex}) incorporated in the EDL, the portion of sodium ions neutralizing the surface charge, and consumption of hydroxide ions have then been deduced from subtracting the total content of sodium and hydroxide remaining in suspensions from that of blank solutions. The estimation of the surface charge density from the pH variations has been done according to the

procedure described in [39]. Shortly, it is the difference between the OH^- added in the suspension and in the blank for a given pH value. These results have been compared to the ones obtained from counter-ions adsorption as described in [40]. In this case, it is the counter-ion amount which is followed (difference between the counter-ions added in the suspension and in the blank) considering that each adsorbed counter-ion balances an ionised site at the surface when the solid is isolated from the dispersion (electroneutrality of the solid). In the present case, the C-S-H counter-ions are both Na^+ and Ca^{2+} but the concentration of the latter is negligible compared to the former and has not been taken into account. Doing so, the error on the surface charge density is less than 5%. We have not used the specific surface area for analysing surface charge experiments, as it is often difficult to measure properly. Instead, the total number of titrating surface sites (silanols) have been determined from the known mass of reactant used to synthesize the C-S-H and stoichiometric considerations. On average, there are two OH functions per three silicon atoms from the known structure and composition of C-S-H. By neglecting the solubility of C-S-H (the solubility corresponds to a few millimolar of silicates compared to more than 200 mM of silicates constituting the C-S-H), one obtain: $\frac{2}{3}\ \frac{m_{SiO_2}}{V \times M_{SiO_2}} = \frac{2}{3}\ \frac{9.724}{0.7915 \times M_{SiO_2}} = 0.136$ mol of silanol groups per liter of suspension.

We consider all silanol groups as identical, that is, no distinction is made between titrating sites situated at the inner or outer surfaces of C-S-H crystallites. Therefore, in each batch used for titration, the total amount of silanol equals: $0.136 \times 34.3 \times 10^{-3} = 4.66 \times 10^{-3}$ mol. Table 1 gives the measured concentrations and pH in each suspension and their corresponding blank solution. The variations of the ionization fractions, calculated by both techniques (titration: $\Delta\alpha(OH)$ and Na^+ adsorption: $\Delta\alpha(Na)$) are also listed.

Electrokinetic potential measurements of C-S-H particles were conducted by electrophoresis using a COULTER DELSA 440 apparatus. C-S-H suspensions used for this purpose were prepared in order to set a liquid to solid ratio of 5000 in weight. The classical Smoluchowski equation has been used to estimate the electrokinetic potential (ζ) from the electrophoretic mobility.

Retention of sodium ion by C-S-H was examined by Viallis et al. [17,28] using the radioactive tracer technique. Sodium chloride solutions were added to C-S-H suspensions (C/S ratios varying from 0.7 to 1.6 and liquid to solid ratio equal 20) so that the initial sodium concentration varied from 10^{-6} to 1 M in the various batches studied. These batches were allowed to equilibrate while shaken for 10 days. After that, 10^{-8} M of ^{22}Na isotope salt was added to the various suspensions. After equilibration for a week, the suspensions were centrifuged at 8000 rpm and the remaining ^{22}Na in the supernatant were titrated by liquid scintillation. The "adsorbed" amount of sodium ions was calculated to be the difference between the total amount of added ^{22}Na and the remaining ^{22}Na in the supernatant for each C-S-H suspension studied.

Note that the usual term "adsorption" does not assume any specific interaction or chemical binding between the ions and the C-S-H surface. It only refers to the ion uptake from the solution to the surface.

Table 1
Data from the titration experiments. The sodium amounts are expressed in quantities (mmol) in the C-S-H suspensions and in the corresponding (same quantity of NaOH added) blank solutions. $\Delta\alpha(Na)$ is the variation of the ionization fraction calculated from the sodium adsorption onto C-S-H. $\Delta\alpha(OH)$ is the variation of the ionization fraction calculated from acid–base titration. See text for other details.

Na_{blank} (mmol)	Na_{susp} (mmol)	$\Delta\alpha$ (Na)	pH_{blank}	pH_{susp}	$\Delta\alpha$ (OH)	$[Ca^{2+}]$ (mM)	[Si] (mM)
0.00	0.00	0.000	10.35	10.35	0.000	1.32	2.50
0.28	0.25	0.006	11.45	10.50	0.000	1.74	3.20
0.53	0.40	0.028	12.10	10.95	0.060	0.40	4.38
0.86	0.53	0.070	12.30	11.45	0.129	0.08	5.28
1.59	0.91	0.145	12.55	12.10	0.225	0.01	2.57
3.99	2.73	0.270	12.80	12.65	0.339	0.003	0.69
11.32	9.35	0.422	13.35	13.00	0.536	0.001	0.37

2.2. Model

2.2.1. Parameters

In our model, the numerous fitting parameters (electric double layer capacitances, effective adsorption constant of ions…) of the classical Stern model [24,25] are reduced to two well-defined parameters, namely the density ρ_N and the ionization equilibrium constant pK_0 of surface sites. More precisely, the intrinsic equilibrium protonation/deprotonation constant of the surface groups is taken to the one of the first deprotonation of silicic acid ($pK_0 = 9.8$) and the surface site density is taken equal to that of the homologue tobermorite structure [27] (4.8 sites/nm²). Beside, the radius of all charged species is set to 2 Å for simplicity reasons. Finally, in agreement with a recent theoretical work of Lund et al. [37] where it was found that the low dielectric interior of a colloid, such as C-S-H, is largely negligible, it is approximated with a uniform high dielectric constant equal to that of the solvent ($\varepsilon_r = 78.6$).

Despite its simplicity, the primitive model is generally found to be extremely robust. Indeed, recently, Abbas et al. [38] performed extensive series of MC simulations in order to explore the validity of the primitive model of electrolyte solutions to describe the bulk thermodynamic properties of real salt solutions. Ionic activity and osmotic coefficients were calculated for 1:1, 2:1 and 3:1 electrolytes by adjusting only the cation radius while keeping the anion radius fixed at its crystallographic value. Unexpectedly, a good agreement between simulations and experiments could be obtained up to few molars for 1:1 salt solutions without the need to reduce the dielectric constant of the liquid medium. In the case of 2:1 and 3:1 salts, the range of validity is more restricted i.e., below few hundreds mM, but still more than enough for the present study and cement systems in general.

A useful parameter that characterizes the ionization state of a surface is the fraction of ionised groups defined as:

$$\alpha = \frac{\sigma}{\rho_N F} \tag{5}$$

where F is the Faraday constant, ρ_N the sites density and σ the surface charge density.

2.2.2. Simulation details

The dimensions of the C-S-H surface were always larger than 100×100 Å² ensuring a total number of sites higher than 400. The third dimension of the simulation box was scaled accordingly, but never less than 100 Å, imposing a number of ions larger than 300. 10^5 moves per mobile particle were attempted in each GCMC run. A method, introducing by Torrie and Valleau [21], is used to treat the long-range contributions of the Coulomb energy in a slab geometry.

During the simulations, the ions are allowed to exchange with a reference bulk solution of set chemical potentials μ_i and thus concentrations c_i. The chemical potentials of all ions (and thus pH) is precomputed in a separate simulation using the modified Widom method [29].

2.2.3. Zeta potential

The electric potential profile in the double layer is calculated from the predicted ion concentration profiles by integrating twice the Poisson equation [25]. The so-called electrokinetic or zeta potential ζ is generally assumed to be equal to the "diffuse potential" [25]. In our simulations, a shift of one and half ion diameter (6 Å) per surface is assumed for the plane where the zeta potential is thought to be measured. It has to be noted that the choice of the latter is not crucial

since the electric potential varies slowly for distances larger than one ion diameter from the C-S-H surface.

Titrations were performed using the experimental conditions at equilibrium i.e., the measured concentrations and pH at equilibrium. In other words, simulations give the amount of adsorbed ions and fraction of ionised site (charge density) for set chemical potential of ions.

Ion adsorption was obtained by summing up (integrating) the excess ion concentration profile at the C-S-H interface.

3. Results

3.1. Surface charge

The simulated increase in the ionization fraction (α) as the pH goes up is illustrated in Fig. 2 for a C-S-H particle next to increasing $Ca(OH)_2$ salt concentration. The ideal curve corresponding to non-interacting sites is given for comparison, in which case 50% of the sites are by definition ionised for $pH = pK_0$. In the case of fully interacting sites (between themselves and with ions in solution) the strong electrostatic repulsion between sites prevents them to be "ideally" ionised. That is a_{Si-O} becomes different from c_{Si-O} and thus the apparent pK of sites (defined by the pH for which $c_{Si-O}/c_{Si-OH} = 1$) is shifted to higher pH value. For the calcium curve a shift of more than 1 pH unit is found. Obviously, the electrostatic interaction between titratable groups depends strongly on the surface site density, salt concentration and valency, suspension concentration as well as the amount of other charged additives, see [19]. As a single example, if it would be possible to replace calcium ion by sodium ion a significant decrease in α would be found, see Fig. 2. This behaviour is mainly explained by the strong ability of the divalent Ca^{2+} counter-ion to compensate (screen) the surface charges. It has been found through MC simulations, not illustrated here, that even a 1 M 1:1 salt would result in a lower surface charge density than 20 mM of a 2:1 salt for the same pH value.

The experimental and simulated titrating curves of a C-S-H dispersion in a 2 mM calcium hydroxide solution are given in Fig. 3. As mentioned before, C-S-H dispersions were chosen to contain a small amount of calcium ions at low pH value, but, even under this condition, the C-S-H surface is partially ionised and hence the complete surface charge titration cannot be determined by experiments alone. That is why the net increase of α ($\Delta\alpha$) instead of α is reported in the figure. A very good agreement is found between simulated and experimental $\Delta\alpha$.

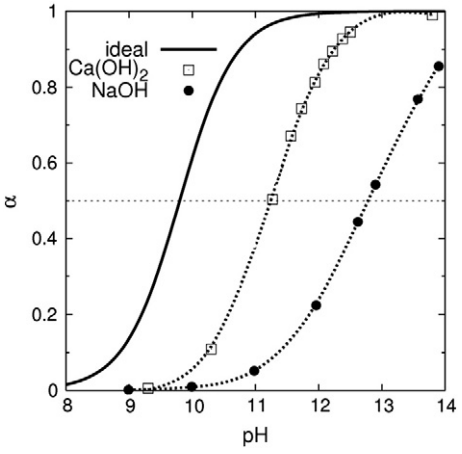

Fig. 2. Simulated ionization fraction, α, versus pH for various bulk conditions: dotted line and squares $Ca(OH)_2$ salt solution; dotted line and filled circles NaOH salt solution. The ideal curve (solid line) is given for comparison.

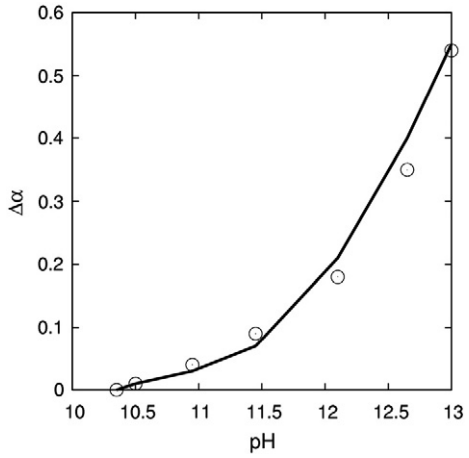

Fig. 3. Comparison between experimental (points) and simulated (line) net increase of the ionization fraction ($\Delta\alpha$) as a function of the pH for C-S-H nano-particles dispersed in solution containing a low bulk calcium concentration.

3.2. Electrokinetic potential

In Fig. 4, the simulated electrostatic profile for a surface next to a bulk electrolyte solution containing $Ca(OH)_2$ salt is plotted. As it can be seen, non-monotonic profiles are found for surfaces at large concentration of $Ca(OH)_2$. Classically, the electrical potential (ϕ) at the surface is negative, having the same sign as the surface charge, and increases for increasing distance from the C-S-H surface, but, for $[Ca(OH)_2] > 2$ mM and at distances larger than ~2 Å (one half diameter of a calcium ion), ϕ reverses its sign and increases further reaching a maximum at ~5 Å. The potential reversal is an increasing function of pH and calcium concentration. In other words, with an increasingly negative surface charge and high calcium concentration, ϕ both becomes more negative at the surface and more positive at few Å from the surface. For such conditions a reversal of the electrokinetic potential measured through electrophoretic measurements is expected.

The predicted and through electrophoretic mobility determined electrokinetic potentials (ζ) as function of the $Ca(OH)_2$ concentration are compared in Fig. 5 for an increasing concentration of $Ca(OH)_2$. A ζ reversal is found at a concentration of ~2 mM of Ca^{2+} as predicted by simulations. However, calculation based on the Poisson–Boltzmann equation (PB) is not able to predict such a behaviour: it gives a uniform negative zeta potential. The agreement between the GCMC simulations and experiments is excellent for the whole range of lime concentration and for various bulk conditions (mixed Na/Ca salt solutions, pH, concentrations) [19].

3.3. Ion retention

Anion adsorption is illustrated in Fig. 7 for a C-S-H surface next to a bulk solution of mixed $CaCl_2/Ca(OH)_2$ salts containing 20 mM Ca^{2+} for varying bulk pH. It is found that the anion adsorption is an increasing function of the pH and calcium concentration. In other words, in the presence of calcium ions, the more the negatively charged surface of C-S-H is high the more anions are adsorbed.

Adsorption isotherms of sodium ions for different C-S-H dispersions have been measured by Viallis et al. [17,28]. Two such isotherms are presented in Fig. 8 for C-S-H dispersion of C/S 0.7 and 1.6 and are compared to GCMC predictions. In the simulations, bulk solution containing a calcium hydroxide concentration of 2 mM and 20 mM for C-S-H having a C/S of 0.7 and 1.6 was assumed, respectively. When increasing the sodium salt concentration, neither experiments nor simulations show saturation of "adsorbed" Na^+ ions. Instead, a linear response (of Freundlish type) is found. What is more, the amount of

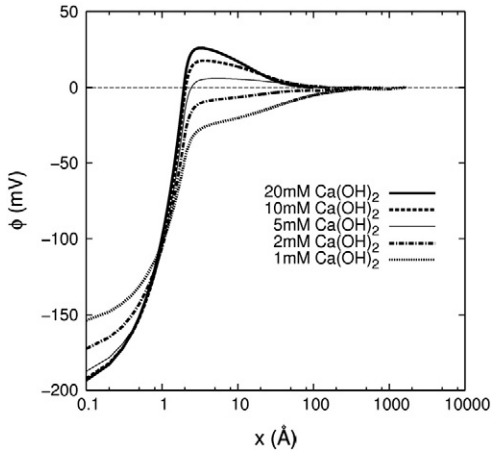

Fig. 4. Electrical potential (ϕ) profile as a function of the distance normal to the C-S-H surface (x) for increasing bulk concentration of $Ca(OH)_2$.

"adsorbed" sodium ions is less for high C/S values, i.e. high surface charge (high pH) and calcium concentration. The experimental results are found to be in good agreement with the GCMC predictions.

4. Discussion

4.1. Surface charge of C-S-H

The first information of importance is that the surface charge of C-S-H is seen from experiments in agreement with the theory (Figs. 2 and 3) to remain negative whatever the calcium concentration and the pH is. At first sight, this result can appear to be in contradiction to the observed reversal of the electrokinetic potential (Fig. 5). We will clarify this apparent discrepancy below. On the other hand, it is in disagreement with the previous statement [11,23,30] that calcium ion is the potential determining ion of cement system (PDI). In this case, one would observe a change in sign of the surface charge of C-S-H. We will develop this issue in the forthcoming paragraph.

The very good agreement found between experiments and theory (Fig. 3) indicates that electrostatic interaction is the main ingredient that cause the titration of individual silanol groups of C-S-H nano-particles leading to the macroscopically and observable surface charge. This means that specific ion adsorptions, if they exist, seem to play a negligible role in the charge formation of C-S-H. Our microscopic approach can, thus, be coupled with our preceding simulations of surface interaction, see [8,9], to predict the interacting force between two C-S-H particles with well-defined physical parameters. Hence, one can have a quick and qualitative picture of the cohesion strength of the final material.

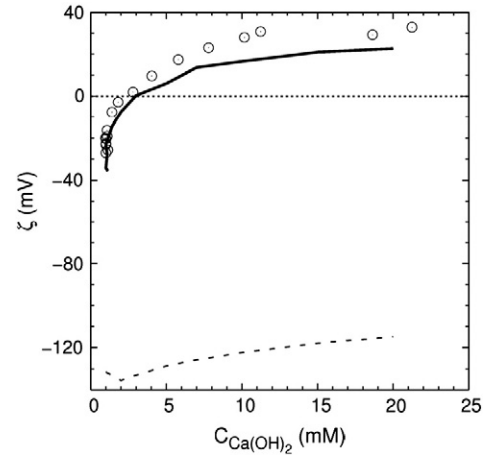

Fig. 5. Zeta potential determined from GCMC (solid curve) and electrophoretic mobility experiments (empty circles) versus bulk $Ca(OH)_2$ for a C-S-H dispersion in pure lime solutions. The results of the mean field theory (dashed curve) are given for comparison.

4.2. Charge reversal

Although the surface charge density of C-S-H remains negative upon addition of lime the reversal of the zeta potential is accurately predicted by our simulations (Figs. 4 and 5). This means that the charge reversal is *apparent*: an ion at x>2 Å feels an electrostatic potential whose sign is opposite to that of the surface, see Fig. 4. Physically, it is explained by an important accumulation of multivalent counter-ions, here calcium, in a thin layer close to the surface of C-S-H which more than neutralised its surface charge and results in its *overcharging*. This phenomenon has been studied in numerous papers [8,10,11,19,31] and is known to be manifestation of charge fluctuations (ion–ion correlations) that occur in the EDL for strong surface charge next to a solution containing multivalent counter-ions. Comparison with zeta potentials, Fig. 5, predicted by the Poisson Boltzmann equation (mean field theory), which, in opposition to experiments, do not exhibit a sign reversal, emphasizes the important role of ion–ion correlations.

Several conclusions can be drawn from these results. Firstly, it confirms that the formal surface charge remains negative, even for the highest lime concentration, while the charge reversal found through electrokinetic measurements is only *apparent*. Indeed, the surface charge becomes more and more negative as the $Ca(OH)_2$ concentration (or pH) is raised, see Fig. 6. The calcium ions are not chemically but physically adsorbed to the C-S-H surface. In other words, most of calcium ions are not bound (chemically bound) to the C-S-H surface but rather closely accumulated to the C-S-H surface due to electrostatic interactions.

Secondly, according to the definition of Hunter and Lyklema [25], adsorbates are best regarded as specifically adsorbed species rather than contributing to the surface charge: they are not potential determining ions (PDI). Consequently, the wide spread idea that calcium is a PDI [11,23,30] in cement paste systems, even though it dramatically affect the activity of the surface sites and thus the surface charge, appears to be incorrect. Instead, the activity of the proton, and thus the pH, controls the charging behaviour of C-S-H nano-particles through the equilibrium Eq. (1). Hence, the proton is the PDI. Note that this is not in contradiction with the fact that the electrostatic interaction between titrable groups, and thus α, depends strongly on the surface site density, salt concentration and valency, suspension concentration as well as the amount of other charged additives.

Finally, we would like to point out that for lime concentrations below 2 mM the surface charge density exhibits an abrupt change, see Fig. 6, while, interestingly, for the same concentration range a phase transition for C-S-H is known to occur [32]. The surface charge density may be the significant physical parameter that drives this phase transition.

4.3. Anion adsorption

A consequence of the build up of an overcompensating counter-ion layer outside the surface as pH increases, is the formation of a co-ion layer at 5–10 Å from the surface, see Fig. 7. The co-ion layer ($Cl^- + OH^-$) neutralizes the overcompensated surface charge of C-S-H by calcium ions. It is promoted by the high surface charge of C-S-H and increases with calcium ion concentration [8,19]. This result qualitatively explains the adsorption of chloride, sulphate and phosphate ions as well as negatively charged polyelectrolytes observed in cement paste and C-S-H dispersion systems [17]. This is of prime interest, since chloride are known for leading great corrosion damaged to reinforcement bars, sulphate for the formation of ettringite and the successive expansion of

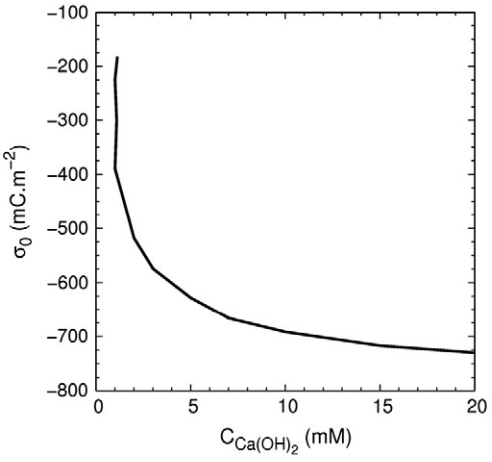

Fig. 6. Predicted surface charge density (σ_0) as a function of the bulk $Ca(OH)_2$ for C-S-H nano-particles dispersed in pure lime solution.

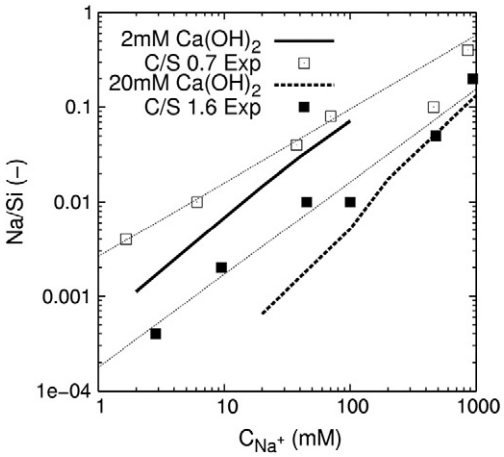

Fig. 8. Experimental and simulated amount of sodium ions "adsorbed" per silica (Na/Si) versus bulk sodium concentration for two C/S ratio and $Ca(OH)_2$/NaCl mixtures. Dotted lines are guides for the eyes.

cement or concrete, and poly-electrolyte for their properties as super-plasticizer. However, it is the first time, to our knowledge, that the anion adsorption in hydrated cement is explained by electrostatic alone, i.e. without invoking the change in sign (from negative to positive) of the C-S-H surface charge and/or the specific chemical adsorption of species.

4.4. Cation adsorption

Again, the electrostatic interactions are the major contribution that drive the cation "adsorption" at the C-S-H/solution interface, see Fig. 8. The observed behaviour of Na^+, non saturating adsorption, is thus the result of the competition of Na^+ and Ca^{2+} in the EDL. That is, when the negative charge of C-S-H is high (high C/S), more sodium ions are needed for replacing the calcium counter-ion and thus less sodium are incorporated in the EDL. This is illustrated in Fig. 9 where the counter-ion concentration profiles are plotted for a C-S-H surface next to a bulk solution for pH 12.48 containing 100 mM NaCl and 20 mM $Ca(OH)_2$. Fig. 9 clearly shows that in the vicinity of the C-S-H surface, for x below ~6 Å, the concentration of the monovalent Na^+ counter-ion is much lower than $c_{Ca^{2+}}$ even if $c_{Na^{2+}}$ is 5 time greater than $c_{Ca^{2+}}$ in the bulk.

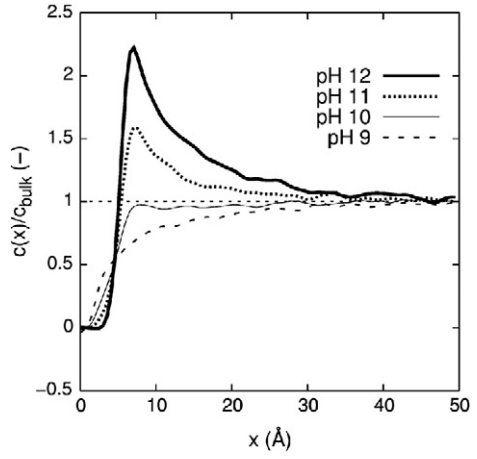

Fig. 7. Simulated monovalent co-ion profile as a function of the distance normal to the surface for C-S-H nano-particles in equilibrium with a bulk solution of mix salts, $Ca(OH)_2/CaCl_2$, containing 20 mM Ca^{2+} and varying the pH value.

4.5. C-S-H stoichiometry

Finally, let us discuss the stoichiometry of C-S-H in terms of measured C/S ratio. We have shown that an *apparent* charge reversal could occur at sufficiently high pH and calcium concentration and it is the result of the overcompensation of the C-S-H charge by an accumulation of calcium counter-ions close to the surface. A question therefore arose: to what extent the electrostatic interactions contribute to the measured C/S ratio? The answer is illustrated in Fig. 10. The results are presented in term of physically "adsorbed" calcium per surface sites (Ca/SiO). For the highest concentration of $Ca(OH)_2$ studied, a Ca/SiO as large as 0.48 is found. One is led to conclude that the electrostatic contribution to measured C/S ratio is important especially for high bulk pH values and calcium concentrations. This means that calcium ions that are physically accumulated at the C-S-H/solution interface cannot be neglected when interpreting measurements of C/S. In other words, measured C/S does not reflect only the chemical composition of C-S-H particles and thus, caution should be used when manipulating such an *apparent* parameter. As an example, S. Garrault [33] has found noticeable decreases of measured C/S ratio when adding large amount of NaCl to C-S-H dispersions. This can be simply explained in terms of electrostatic interactions — see above. On the other hand, the high C/S (>1.5) of C-S-H found by Nonat and Lecoq [33–35] cannot be explained by electrostatics alone.

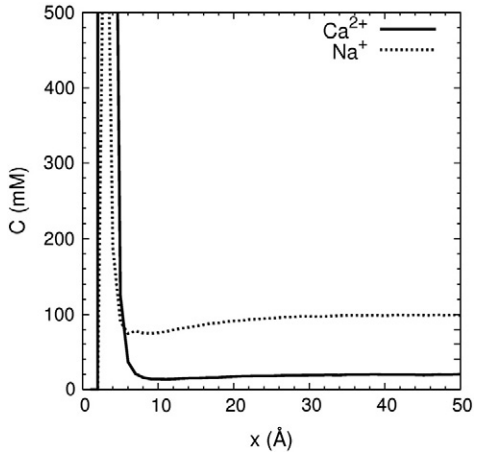

Fig. 9. Simulated counter-ion concentration profiles for a C-S-H surface next to a bulk solution containing 20 mM $Ca(OH)_2$ and 100 mM NaCl at pH 12.48.

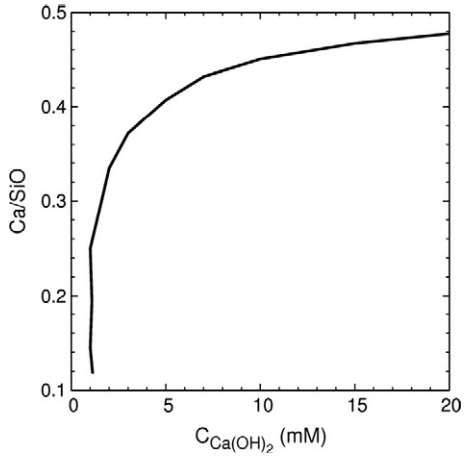

Fig. 10. Simulated amount of calcium "adsorbed" per silanol group of C-S-H as a function of the bulk $Ca(OH)_2$ concentration.

5. Conclusion

In this work, we have reported results from grand canonical Monte Carlo simulations of the surface charge density, ionic adsorption isotherm and electrokinetic potential of C-S-H particles in equilibrium with various electrolyte solutions. In these simulations, the C-S-H surface is modelled by explicit ionizable surface sites, mimicking the protonation and deprotonation of silanol groups, distributed on a square lattice surface. Only two parameters are needed in order to describe the surface titration, namely an intrinsic dissociation constant and a surface site density. The density and the intrinsic dissociation constant have been taken equal to that of the homologue tobermorite structure (4.8 sites/nm^2) and that of the first ionization of silisic acid ($pK_a = 9.8$), respectively.

Computed and experimental data of C-S-H dispersion titration have been compared. Results from both experiments and simulations are in very good agreement with only two well-defined physical parameters. This indicates that our theoretical approach has a sound physical basis.

GCMC simulations have allowed us to predict quantitatively the sign reversal of ζ observed through electrophoretic measurements of C-S-H dispersions in lime solution of varying concentration. The sign reversal of ζ, often interpreted as *charge reversal,* is, in fact, caused by strong physical adsorption of calcium ions in the vicinity of the C-S-H surface induced by ion–ion correlations which leads to an overcompensation of the *still negative* surface charge density, e. g. the charge reversal is *apparent*. The affinity of calcium ions for the C-S-H particles is the result of the electrostatic interactions alone: *no specific chemical adsorption* occurs. As a consequence, the increase in the C/S ratio of C-S-H with increasing lime concentration can be explained, until C/S = 1.5, without invoking a specific binding of calcium ions.

Such a surface behaviour may be extended to the case of tri-calcium-silicate surface as well. As a matter of fact before dissolution and as soon as the surface is in contact with water, surface SiO_4^{4-} are hydroxylated [33,34,36] and C_3S surface presents then a silanol surface density close to C-S-H. That is why, while it is not yet hydrated, the electrokinetic behaviour of C_3S suspensions in lime solutions is the same as C-S-H suspensions [28,30].

Finally good agreement is found between experimental and predicted adsorption isotherm of sodium for various $NaCl/Ca(OH)_2$ electrolyte mixtures. This leads us to expect that our theoretical approach can be useful for the prediction of the cement ability to retain pollutions such as heavy metal ions. Same kind of work concerning the predicted adsorption of anions and polyelectrolytes isotherms is in progress and will be published in a foregoing paper.

References

[1] S.P. Jiang, J.C. Mutin, A. Nonat, Studies on mechanism and physico-chemical parameters at the origin of the cement setting, I. The fundamental processes involved during the cement setting, Cement and Concrete Research 25 (1995) 779.
[2] S.P. Jiang, J.C. Mutin, A. Nonat, Studies on mechanism and physico-chemical parameters at the origin of the cement setting, II. Physico-chemical parameters determining the coagulation process, Cement and Concrete Research 26 (1996) 491.
[3] S. Lesko, E. Lesniewska, A. Nonat, J.-C. Mutin, J.-P. Goudonnet, Investigation by atomic force microscopy of forces at the origin of cement cohesion, Ultramicroscopy 86 (2001) 11.
[4] L. Nachbaur, J.C. Mutin, A. Nonat, L. Choplin, Dynamic mode rheology of cement and tricalcium silicate pastes from mixing to setting, Cement and Concrete Research 31 (2001) 183.
[5] C. Plassard, E. Lesniewska, I. Pochard, A. Nonat, Nanoscale experimental investigation of particle interactions at the origin of the cohesion of cement, Langmuir 21 (2005) 7263.
[6] S. Meyer, A. Delville, Monte Carlo study of the electrostatic forces between charged lamellae: influence of surface charge localisation, Langmuir 17 (2001) 7433.
[7] R.J.-M. Pellenq, J.M. Caillol, A. Delville, Electrostatic attraction between two charged surfaces: a (N, V, T) Monte Carlo simulation, Journal of Physical Chemistry B 101 (1997) 8584.
[8] B. Jönsson, A. Nonat, C. Labbez, B. Cabane, H. Wennerstrom, Controlling the cohesion of cement paste, Langmuir 21 (2005) 9211.
[9] B. Jönsson, H. Wennerstrom, A. Nonat, B. Cabane, Onset of cohesion in cement paste, Langmuir 20 (2004) 6702.
[10] L. Guldbrand, B. Jönsson, H. Wennerstrom, P. Linse, Electrical double layer forces: a Monte Carlo study, Journal of Chemical Physics 80 (1984) 2221.
[11] R. Kjellander, S. Marcelja, Correlation and image charge effects in electric double layers, Chemical Physics Letters 112 (1984) 49.
[12] L. Nachbaur, P.-C. Nkinamubanzi, A. Nonat, J.C. Mutin, Electrokinetic properties which control the coagulation of silicate cement suspensions during early age hydration, Journal of Colloid and Interface Science 202 (1998) 261.
[13] P. Fievet, C. Labbez, A. Szymczyk, A. Vidonne, A. Foissy, J. Pagetti, Electrolyte transport through amphoteric nanofiltration membranes, Chemical Engineering Science 57 (2002) 2921.
[14] Y. Maltais, J. Marchand, P. Henocq, T. Zhang, J. Duchesne, Importance of physical and chemical interactions in presence of chloride or sulfate ions, in: J. Skalny (Ed.), Materials Science of Concrete VII, The American Ceramic Society, 2004.
[15] J. Marchand, E. Samson, D. Burke, P. Tourney, N. Thaulow, S. Sahu, Predicting the microstructural degradation of concrete in marine environment, ACI special publication SP-212, 2003, p. 1127.
[16] A. Szymczyk, C. Labbez, P. Fievet, A. Vidonne, A. Foissy, J. Pagetti, Contribution of convection, diffusion and migration to electrolyte transport through nanoflitration membranes, Advances in Colloid and Interface Science 103 (2003) 77.
[17] H. Viallis, P. Faucon, J.-C. Petit, A. Nonat, Interaction between salts (NaCl, CsCl) and calcium silicate hydrates (C-S-H), Journal of Physical Chemistry B 103 (1999) 5212.
[18] A.-E. Yaroshchuk, Y.-P. Boiko, A.-L. Makovetskiy, Some properties of electrolyte solutions in nanoconfinement revealed by the measurement of transient filtration potential after pressure switch off, Langmuir 21 (2005) 7680.
[19] C. Labbez, B. Jönsson, I. Pochard, A. Nonat, B. Cabane, Surface charge density and electrokinetic potential of highly charged minerals: experiments and Monte Carlo simulations on calcium silicate hydrate, Journal of Physical Chemistry B 110 (2006) 9219.
[20] W.V. Megen, I. Snook, The Grand Canonical ensemble Monte Carlo method applied to the electric double layer, Journal of Chemical Physics 73 (1980) 4656.
[21] G.M. Torrie, J.P. Valleau, Monte Carlo study of a uniformly charged surface, Journal of Chemical Physics 73 (1980) 5807.
[22] M.P. Allen, D.J. Tildesley, Computer Simulation of Liquids, Oxford Science, 2001.
[23] P. Henocq, Modélisation des interactions ioniques à la surface des silicates de calcium hydratés, PhD thesis, Laval University and University of Cergy-Pontoise, Quebec and Cergy-Pontoise.
[24] T. Hiemstra, W.H. Van Riemsdjik, G.H. Bolt, Multisite proton adsorption modelling at the solid/solution interface of (hydr)oxides: a new approach: I. model description and evaluation of intrinsic reaction constants, Journal of Colloid and Interface Science 131 (1989) 91.
[25] R.J. Hunter, Fundations of Colloid Science, E. C. Press, 1995.
[26] T. Kesvatera, B. Jönsson, E. Thulin, P. Linse, Ionisation behaviour of acidic residues in calbindin D9k, Proteins 37 (1997) 106.
[27] S.A. Hamid, The crystal structure of the 11 Å natural tobermorite $Ca_{2.25}[Si_2O_{7.5}(OH)_{1.5}]$, $11H_2O$, Zeitschrift fur Kristallograhie 154 (1981) 189.
[28] H. Viallis, Interaction des silicates de calclium hydratés, principaux consitutants du ciment, avec les chlorures d'alcalins. Analogie avec les argiles, PhD thesis, University of Bourgogne, Dijon, (2000).
[29] B.R. Svensson, C.E. Woodward, Widom's method for uniform and non-uniform electrolyte solutions, Molecular Physics 64 (1988) 247.
[30] H. Viallis-Terrisse, A. Nonat, J.-C. Petit, Zeta-potential study of calcium silicate hydrates interacting with alkaline cations, Journal of Colloid and Interface Science 244 (2001) 58.
[31] L. Sjöström, T. Akesson, B. Jönsson, Charge reversal in electric double layers — a balance between energy and entropy, Berichte der Bunsen-Gesellschaft für Physikalische Chemie 100 (1996) 889.
[32] P.S. Roller, G. Ervin, The system calcium oxide–silica–water at 30 °C. The association of silicate ion in dilute alkaline solution, Journal of the American Chemical Society 62 (1940) 461.

[33] S. Garrault-Gauffinet, Etude expérimentale et par simulation numérique de la cinétique de croissance et de la structure des hydrosilicates de calcium, produits d'hydratation des silicates tricalcique et dicalcique, PhD thesis, University of Bourgogne, Dijon, (1998).
[34] D. Damidot, F.P. Glasser, Thermodynamique investigation of the $CaO–Al_2O_3–CaSO_4–CaCO_3–H_2O$, Advances in Cement Research 7 (1995) 129.
[35] A. Nonat, X. Lecoq, Nuclear Magnetic Resonance Spectroscopy of cement based materials, Bergamo, Italie, 1996.
[36] P. Barret, Sur l'existence d'un stade d'hydroxylation superficielle dans le processus de dissolution du silicate tricalcique et son influence sur la solubilité de ce consitutant du ciment, Compte Rendu de l'Académie des Sciences 288 (1979) 461.
[37] M. Lund, B. Jönsson, C.E. Woodward, Implication of a high dielectric constant in proteins, Journal of Chemical Physics 126 (2007) 225103.
[38] Z. Abbas, E. Ahlberg, S. Nordholm, Monte Carlo simulations of salt solutions: exploring the validity of primitive models, Journal of Physical Chemistry C 113 (2009) 5905.
[39] W. Stumm, Chemistry of the Solid–Water Interface, Wiley-Interscience, New York, 1992.
[40] I. Pochard, J.P. Boisvert, C. Daneault, Donnan equilibrium and the effective charge of sodium poly(acrylate), Colloid and Polymer Science 279 (2001) 850–857.